2010

Acetyl-L-carnitine protects neuronal function from alcohol-induced oxidative damage in the brain

Travis J. Rump
University of Nebraska Medical Center

P. M. Abdul Muneer
University of Nebraska Medical Center

Adam M. Szlachetka
University of Nebraska Medical Center

Allyson Lamb
University of Nebraska Medical Center

Catherine Haorei
University of Nebraska Medical Center

See next page for additional authors

Free Radical Biology & Medicine 49 (2010) 1494–1504

Contents lists available at ScienceDirect

Free Radical Biology & Medicine

journal homepage: www.elsevier.com/locate/freeradbiomed

Original Contribution

Acetyl-L-carnitine protects neuronal function from alcohol-induced oxidative damage in the brain

Travis J. Rump [a], P.M. Abdul Muneer [a], Adam M. Szlachetka [a], Allyson Lamb [a], Catherine Haorei [a], Saleena Alikunju [a], Huangui Xiong [a], James Keblesh [a], Jianuo Liu [a], Matthew C. Zimmerman [b], Jocelyn Jones [b], Terrence M. Donohue Jr. [c], Yuri Persidsky [d], James Haorah [a,*]

[a] Department of Pharmacology and Experimental Neuroscience, University of Nebraska Medical Center, Omaha, NE 68198, USA
[b] Department of Cellular and Integrative Physiology, University of Nebraska Medical Center, Omaha, NE 68198, USA
[c] Department of Internal Medicine and Veterans Affairs Medical Center, Omaha, NE 68105, USA
[d] Department of Pathology and Lab Medicine, Temple University School of Medicine, Philadelphia, PA 19140, USA

ARTICLE INFO

Article history:
Received 21 January 2010
Revised 17 July 2010
Accepted 5 August 2010
Available online 12 August 2010

Keywords:
Acetyl-L-carnitine
Alcohol-induced oxidative damage
Neurodegeneration
Astrogliosis
Synaptic neurotransmission
Free radicals

ABSTRACT

The studies presented here demonstrate the protective effect of acetyl-L-carnitine (ALC) against alcohol-induced oxidative neuroinflammation, neuronal degeneration, and impaired neurotransmission. Our findings reveal the cellular and biochemical mechanisms of alcohol-induced oxidative damage in various types of brain cells. Chronic ethanol administration to mice caused an increase in inducible nitric oxide synthase (iNOS) and 3-nitrotyrosine adduct formation in frontal cortical neurons but not in astrocytes from brains of these animals. Interestingly, alcohol administration caused a rather selective activation of NADPH oxidase (NOX), which, in turn, enhanced levels of reactive oxygen species (ROS) and 4-hydroxynonenal, but these were predominantly localized in astrocytes and microglia. Oxidative damage in glial cells was accompanied by their pronounced activation (astrogliosis) and coincident neuronal loss, suggesting that inflammation in glial cells caused neuronal degeneration. Immunohistochemistry studies indicated that alcohol consumption induced different oxidative mediators in different brain cell types. Thus, nitric oxide was mostly detected in iNOS-expressing neurons, whereas ROS were predominantly generated in NOX-expressing glial cells after alcohol ingestion. Assessment of neuronal activity in *ex vivo* frontal cortical brain tissue slices from ethanol-fed mice showed a reduction in long-term potentiation synaptic transmission compared with slices from controls. Coadministration of ALC with alcohol showed a significant reduction in oxidative damage and neuronal loss and a restoration of synaptic neurotransmission in this brain region, suggesting that ALC protects brain cells from ethanol-induced oxidative injury. These findings suggest the potential clinical utility of ALC as a neuroprotective agent that prevents alcohol-induced brain damage and development of neurological disorders.

Published by Elsevier Inc.

Evidence indicates that millions of chronic alcohol abusers exhibit neuronal injury and neurocognitive deficits associated with neuronal degeneration [1–3]. Although oxidative damage has been implicated in many neurological diseases such as Alzheimer disease, Parkinson disease, amyotrophic lateral sclerosis, and stroke [4,5], the underlying mechanisms of alcohol-induced neuropathology remain elusive. There are multiple mechanisms of alcohol-induced neurotoxicity and neuronal degeneration in various brain regions [6]. Thus, ethanol-elicited reactive gliosis in hippocampus and cortex clearly indicate the role of free radical formation in young and aged rats [7]. Findings by Pierce et al. [8] do not support the role of robust oxidative mechanisms as the primary cause of Purkinje cell death in the cerebella of neonatal rats. However, other findings indicate that microglial activation, enhanced neuroinflammation, and oxidative damage occur before brain atrophy after chronic alcohol ingestion [9,10]. These findings support the notion that oxidant generation is a cause of neuroinflammation and neuronal degeneration in alcoholics. Recent findings in postmortem alcoholic human brain tissues [11] and in animal models [9,12] also indicate that alcohol-induced astrogliosis causes neuroinflammation.

Recently, Crews and Nixon [13] demonstrated the mechanisms of alcohol-induced oxidative stress and proinflammatory protein products that trigger neurodegeneration during alcohol intoxication. Furthermore, Sullivan and Zahr [14] extensively described neuropathological, neuroelectrophysiological, neuropsychological, and neuroradiological evidence for alcohol-induced neuronal loss in humans. We and others have demonstrated the biochemical and molecular mechanisms of alcohol-induced oxidative production as contributing factors to neuronal degeneration after alcohol-induced breaching of

* Corresponding author. Fax: +1 402 559 8922.
E-mail address: jhaorah@unmc.edu (J. Haorah).

0891-5849/$ – see front matter. Published by Elsevier Inc.
doi:10.1016/j.freeradbiomed.2010.08.011

brain microvascular endothelial cells [15,16], brain astrocytes [17,18], and cultured microglia [19]. We reported a significant induction of cytochrome P450-2E1 activity, which was associated with increased levels of reactive oxygen species (ROS) and nitric oxide (NO) production in human neurons after exposure to 17.5 mM ethanol (EtOH) [17]. These findings indicate that ethanol metabolism and subsequent reactive oxidant production by both NADPH oxidase (NOX) and inducible nitric oxide synthase (iNOS) significantly contribute to oxidative stress in the central nervous system (CNS).

In biological systems, products of oxidative reactions are broadly classified as ROS. Major forms of ROS include superoxide anion ($O_2^{\bullet-}$), hydroxyl radical ($^{\bullet}OH$), hydrogen peroxide (H_2O_2), hypochlorous acid, and alkoxyl and peroxyl radicals. Reactive nitrogen species (RNS) include the nitric oxide radical and peroxynitrite. ROS ($O_2^{\bullet-}$ and $^{\bullet}OH$) are produced by normal mitochondrial oxidative phosphorylation, by conversion of l-arginine to l-citrulline catalyzed by NOX/xanthine oxidase, and from nonenzymatic Fenton–Haber–Weiss reactions of H_2O_2 that occur during reduction of iron. Conversion of l-arginine to l-citrulline, when catalyzed by calcium/calmodulin-independent iNOS and -dependent eNOS (endothelial, constitutive) or nNOS (neuronal, constitutive), produces the short-lived NO. Nitric oxide reacts with superoxide to form the highly reactive radical peroxynitrite. This RNS can covalently conjugate with reactive amino acids (e.g., tyrosine) in proteins and alter their biological properties.

In this study, we investigated the therapeutic efficacy of acetyl-L-carnitine (ALC) administration in a mouse model of chronic alcohol feeding. We postulated that administration of ALC would restore antioxidant levels and improve mitochondrial function, neurotransmission, and neuronal survival in the brains of ethanol-fed mice. ALC is a naturally occurring neuroprotective agent that delivers carnitine and acetyl groups in clinical therapeutic settings, currently used for treatment of strokes and Alzheimer disease [20,21]. ALC acts as the transporter of long-chain fatty acid (FA) into, and small/medium-chain FA out of, mitochondria. It is an effective antioxidant and neurotransmitter and a potent inhibitor of excitotoxicity. ALC is expected to maintain the normal coenzyme A (CoQ10) level and oxidative phosphorylation balance within mitochondria. CoQ10 itself is a neuroprotective agent and antioxidant, found predominantly in mitochondria, where it maintains and stabilizes the mitochondrial membrane potential under conditions of oxidative stress. Administration of ALC mitigates the age-related decay of mitochondrial function [22] and increases choline acetyltransferase activity (cholinergic neuronal activity) in rat hippocampus [23]. We hypothesized that ALC administration in our animal model would improve neurotransmission and neuronal survival by suppressing generation of biological oxidants thereby stabilizing dopaminergic and cholinergic neurons in the brain. Our findings indeed demonstrate therapeutic benefits of ALC in preventing alcohol-induced neurodegeneration, the results of which are reported here.

Materials and methods

Animal procedures

To evaluate the effects of chronic feeding of ethanol liquid diets in a mouse model, 5-week-old C57BL/6 J male mice were purchased from The Jackson Laboratory (Bar Harbor, ME, USA) and maintained in the University of Nebraska Medical Center animal facility, following the NIH *Guide for the Care and Use of Laboratory Animals.* Five days before actual pair-feeding, all mice were fed the control liquid diet for 2 days and then alcohol-diet-fed mice were acclimated to 28% EtOH (4% vol/vol, or 870 mM) liquid diet (as percentage of total calories) for 3 days. Animals were then pair-fed the control or the ethanol liquid diet for 8 weeks (pair-feeding was based on ethanol diet consumption) in the following groups: pair-fed control, EtOH-fed, pair-fed EtOH + ALC, pair-fed EtOH + CoQ10, and pair-fed ALC alone (eight mice/group, or three mice/basal control of ALC or CoQ10). The macronutrient composition of the control Lieber–DeCarli diet from Dyets, Inc., in percentage of total calories is 47% carbohydrate, 35% fat, and 18% protein, whereas the EtOH liquid diet is 35% fat, 18% protein, 19% carbohydrate, and 28% ethanol. ALC was mixed in liquid diets (2 mg/ml), whereas CoQ10 (2 mg/g body wt) was administered in saline solution by daily intraperitoneal (ip) injection. After 8 weeks, the mice were euthanized by ip injection of ketamine (800 mg/kg). Blood was removed from all mice for determination of alcohol levels (determined by EtOH assay kit; Diagnostic Chemicals Ltd, Charlottetown, PEI, Canada). Whole-brain tissue weights were recorded before dissecting into frontal or caudal (without cerebellum) cortical regions for histopathology. Brains were fixed in 4% paraformaldehyde and preserved in OCT for immunohistochemistry. Tissues were stored at −80 °C for protein or RNA extraction.

Western blot

Protein extracts from brain frontal cortex homogenates were centrifuged at 12,000 rpm for 20 min. Supernatants were diluted in sample buffer, heated at 95 °C for 3–5 min, and subjected to denaturing (SDS) electrophoresis by loading 20 μg protein/lane on precast 4–15% gradient polyacrylamide gels. Molecular-size-separated proteins on gels were transferred onto nitrocellulose membranes at room temperature for 1 h at 60 V. After being blocked with Superblock T-20 (Thermo Scientific, Rockford, IL, USA) containing 2% nonfat dry milk, membranes were incubated overnight with primary antibody against iNOS (ab3523, 1:1000), 3-nitrotyrosine (3-NT; ab52309, 1:1000), NOX1 (ab55831, 1:200) (Abcam, Cambridge, MA, USA); 4-hydroxynonenal (4-HNE; 1:1000; HNE11-S, Alpha Diagnostic, San Antonio, TX, USA); or α-actin (1:1000; Millipore, Billerica, MA, USA) protein at 4 °C followed by 1 h incubation with horseradish peroxidase-conjugated secondary antibodies at room temperature. The negative controls such as blocking reagent and secondary antibody were used to check the specificity of the immunoblot. Immunoreactive bands were detected by West Pico chemiluminescence substrate (Thermo Scientific) using the autoradiography developer. Data were quantified as arbitrary densitometry intensity units using the Gelpro32 software package (version 3.1; Media Cybernetics, Marlow, UK).

Immunofluorescence and microscopy

Immunohistochemistry was performed on 5-μm brain tissue coronal sections. Tissue sections were washed with phosphate-buffered saline (PBS) and fixed in acetone and methanol (1/1 vol/vol) and were blocked at room temperature in PBS containing blocking serum (3% bovine serum albumin; BSA). Tissues were then incubated with respective primary antibodies (Abcam) such as 3-NT (ab61392, ab78406, 1:200), iNOS (ab3523, 1:50), NOX1 (ab55831, 1:150), tyrosine hydroxylase (TH; ab113, 1:1000), or choline acetyltransferase (ChAT; ab18736, 1:1000) with 0.4% Triton X-100 overnight at 4 °C. Antibodies to NeuN (ab77315; 1:250), neurofilaments (ab28029; 1:100), GFAP (ab7260, ab10062, 1:250), and Iba1 (ab5076, 1:100) were used for detection of neuronal nucleus and cytoplasm, neurofilaments, astrocytes, and microglia, respectively, in brain tissue sections. After being washed with PBS, tissue sections were incubated with the secondary antibody (Alexa Fluor 488 and Alexa Fluor 594; Invitrogen; 1:500) for 1 h. Blocking sera (BSA) without primary/secondary antibodies and secondary antibody without primary antibody were used as negative controls to detect the specificity of immunofluorescence. Immunohistochemical studies for all marker proteins were mounted in Immunomount containing DAPI to stain nuclei (Invitrogen). Tissue sections were analyzed by fluorescence microscope (Eclipse TE2000-U; Nikon, Melville, NY, USA) connected to a color DigFire digital camera (Photometrics Cool Snap EZ, Goleta, CA, USA).

ROS detection

Brain tissues from the various treatment conditions were washed in KDD buffer and cut into pieces with nonmetallic (plastic) scalpel, and tissues (100 mg/tube) were suspended in spin-probe solution for detection of ROS and RNS. Tissues were totally submerged in the spin-probe solution (1.0 ml) in Eppendorf tubes before incubation at 37 °C for 30–60 min. Samples aspirated in a 1.0-ml syringe were snap-frozen in liquid nitrogen until detection of ROS by electron paramagnetic resonance (EPR; Bruker Escan E-box tabletop model, Serial 0264) within 1 h. The EPR was set at field sweep in lagtime that read 10×10 scans for an accumulative, or a "time course" protocol: microwave bridge → attenuator 4.0 for liquid samples, 17 for frozen samples; number of scans per sample 10; hall → center field 3450.189 Gauss (G), sweep width 60 G, static field 3451.189 G. Krebs Hepes buffer contains 99 mM NaCl, 4.69 mM KCl, 2.5 mM $CaCl_2 \cdot 2H_2O$, 1.2 mM $MgSO_4 \cdot 7H_2O$, 25 mM $NaHCO_3$, 1.03 mM KH_2PO_4, 5.6 mM d-(+)-glucose, and 20 mM Na-Hepes. KDD buffer consists of the Krebs Hepes buffer and the chelators DF (25 μM) and DETC (5 μM). We used the spin-probe solution CMH (Noxygen, NOX-2.3–100 mg; Axxora ALX-430-117-M010) in KDD buffer, which reacted with intracellular superoxide. The nonspecific free radical measurement was corrected by subtracting the arbitrary units of 10 mM specific scavenged condition, such as mannitol (Sigma M9647, Sigma B3420) for hydroxyl radicals, superoxide dismutase (Sigma G001835) for superoxide, and cPTIO (Sigma C221) for nitric oxide, from the unscavenged experimental conditions. Data are presented as cumulative detection of both the hydroxyl and the superoxide free radicals. TEMPOL and H_2O_2 were used as positive controls for the presence of free radicals.

Electrophysiology recordings

We then studied the long-term potentiation (LTP) synaptic transmission of neuronal activity in ex vivo frontal cortical brain tissue slices by electrophysiology. Briefly, three mice each from control, EtOH, and EtOH + ALC as described above were used for electrophysiological recordings at week 7 to 8. Brains removed from the cranial cavity were placed into ice-cold (4 °C) preoxygenated artificial cerebrospinal fluid (ACSF). Frontal cortex transverse ex vivo brain slices (400 μm in thickness) were prepared using a tissue chopper after a previously published method [24]. Slices were kept in a humidified/oxygenated holding chamber at room temperature for at least 1 h before being transferred to a recording chamber. In the recording chamber, a single frontal cortex slice was submerged and perfused continuously (2.0 ml/min) with ACSF containing 124 mM NaCl, 3 mM KCl, 2 mM $CaCl_2$, 2 mM $MgCl_2$, 1 mM NaH_2PO_3, 26 mM $NaHCO_3$, and 10 mM glucose equilibrated with 95% O_2 and 5% CO_2, pH 7.35–7.45. The perfusate temperature was maintained at 30 ± 1 °C with an automatic temperature controller (Warner Instrument Corp., Hamden, CT, USA).

Field excitatory postsynaptic potentials (fEPSPs) were elicited by a constant current stimulation (0.05 Hz, 100–300 μA, test pulses) of Schaffer collateral-commissural axons using an insulated bipolar tungsten electrode. Intensity and duration of stimulation were adjusted to generate approximately 50% of the maximal response. Evoked fEPSPs were recorded with an Axopatch-1D amplifier (Molecular Devices, Sunnyvale, CA, USA) in the CA1 dendrite field (stratum radium). Recordings were made with borosilicated glass microelectrodes with a tip diameter of 2.5–5.0 μm and a resistance of 1–5 MΩ when filled with ACSF. A 15- to 20-min control (baseline) recording was conducted in each experiment once the adjustment of stimulation parameters was achieved. Electrical signals were filtered at 1 kHz and digitized at a frequency of 2.5 kHz using a Digidata 1320 interface (Molecular Devices). Data were stored on a desktop PC and analyzed offline using pCLAMP 10 software (Molecular Devices).

Table 1
Body and brain weights and blood alcohol levels in alcohol-fed mice

Condition	Body weight (g)	Brain weight (g)	Brain weight expressed in mg/g body wt	Blood alcohol level (mM)
Control	22.78 ± 2	0.427 ± 0.01	19.0	0.0 ± 0.003
EtOH	24.47 ± 2	0.404 ± 0.02	16.5	17.6 ± 3.77
EtOH + ALC	22.88 ± 2	0.413 ± 0.01	18.0	10.8 ± 2.05
EtOH + CoQ10	23.73 ± 2	0.402 ± 0.01	17.0	10.2 ± 1.75
ALC	24.89 ± 2	0.414 ± 0.02	16.6	0.0 ± 0.002

Initial slope of the EPSPs was expressed as percentage of basal level, which is the average of the initial slopes of the first 5 min.

Statistical analysis

Results are expressed as mean values (±SD), and a probability value of ≤0.05 was considered significant. Statistical significance was assessed by two-way ANOVA analyses with Newman–Keuls posttest for multiple comparisons.

Results

The average body weight of ethanol-fed mice was significantly higher ($p<0.02$; $N=8$) than that of pair-fed controls or mice in the

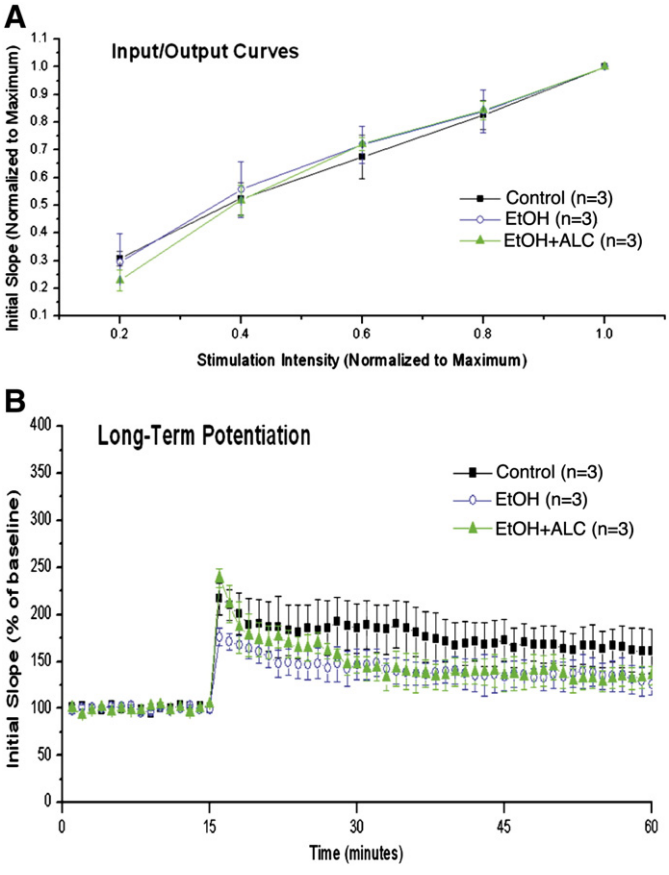

Fig. 1. ALC prevented alcohol-induced reduction in LTP synaptic transmission in frontal cortex tissue slice. LTP synaptic responses were induced by a constant current stimulation (twin pulses, 150–300 μA, 40 μs, 0.05 Hz) of Schafer collateral fibers in three conditions. The graphs plot the initial slope of the first evoked excitatory postsynaptic potentials recorded from the frontal cortex in response to constant current stimuli. Synaptic transmission in the frontal cortex region of mouse brain slices is shown. (A) Input and output curves. (B) Pair-fed control mice, EtOH liquid diet, EtOH liquid diet with ALC supplementation. Results are expressed as mean values of three mice per group (±SD; $n=3$).

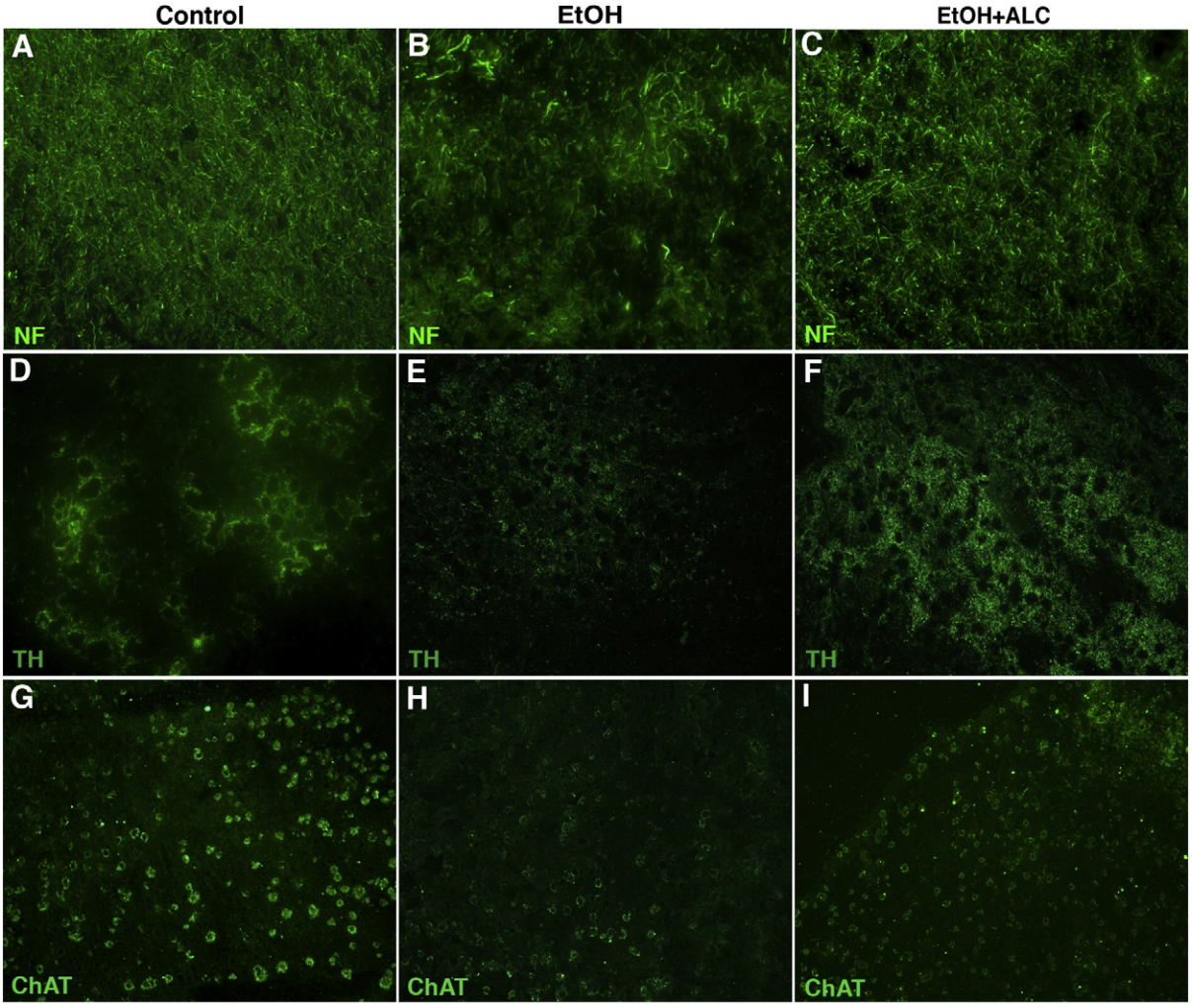

Fig. 2. ALC administration protected frontal cortical neurons from depletion of NF from chronic alcohol feeding. (A–C) Immunohistochemical staining for marker protein (neurofilaments, NF) on 5-μm tissue sections from (A) control, (B) EtOH, and (C) EtOH + ALC conditions. Neurofilaments were immunolabeled with antibody to NF (mouse IgG, 1:100; Abcam ab28029) for 1 h at 24 °C. Alexa Fluor 488 anti-mouse secondary antibody was used for conjugation and fluorescence detection of neurofilaments (green). (D–F) Expression of dopaminergic neuronal marker protein tyrosine hydroxylase (TH, green) in (D) control, (E) EtOH, and (F) EtOH + ALC. (G–I) Cholinergic neuronal marker protein choline acetyltransferase (ChAT, green) in (H) control, (I) EtOH, and (J) EtOH + ALC. TH (sheep IgG, 1:1000; Abcam ab113) and ChAT (sheep IgG, 1:1000, Abcam ab18736) were used as primary antibodies for these stainings. Alexa Fluor 488 anti-sheep secondary antibody was used for both TH and ChAT. Original magnification, ×20.

alcohol + ALC group. Conversely, the mean weight of whole-brain tissue of alcohol-fed mice was lower than that of the control or alcohol + ALC group after 8 weeks of liquid diet administration (see Table 1). The average amount of intake per animal was about 17.0 ml during the control liquid diet acclimation period. The pattern of food intake during pair-feeding was about 12, 15, 16, and 18 ml/mouse, respectively, at week 1, 2, 3, and 4–8. Pair-feeding of all other conditions was based on the volume of EtOH liquid diet intake in the alcohol condition.

Alcohol-fed animals exhibited behavioral changes during the ethanol period. We observed that these animals were physically less active and were less alert compared with the pair-fed control or the alcohol-diet plus ALC animals. We speculated that the change in behavior was related to impairment of synaptic transmission resulting from alcohol-induced oxidative damage and mitochondrial energy depletion, leading to loss of neuronal activity. Thus, we analyzed the low-frequency stimulus (LFS) and LTP synaptic transmission of neuronal activity in ex vivo frontal cortical brain tissue slices. These analyses revealed a significant reduction in LTP and LFS synaptic transmission in the CA1 region in brain slices from alcohol-fed mice compared with pair-fed controls (Figs. 1A and B). As anticipated, ALC prevented the alcohol-elicited loss of LTP and LFS synaptic transmission in the frontal cortex, suggesting that ALC blocked the loss of neuronal activity, perhaps by stabilizing mitochondrial function. These data are consistent with our recent findings that, in culture, ALC exposure protects primary human neurons from EtOH/Acetaldehyde (Ach) insult [17].

To evaluate the neuroprotective effects of ALC in our animal model, we first examined the changes in the expression of neuronal marker protein neurofilament (NF) in frontal cortex coronal sections by immunofluorescence, using antibody to neurofilament protein. The data indicated that ethanol administration diminished NF fluorescence in cortical sections. However, daily coadministration of ALC with ethanol liquid diet prevented the loss of NF from cortical neurons in these animals (Figs. 2A–C). The mitochondrial-specific antioxidant CoQ10 afforded very minimal neuroprotection from chronic alcohol administration (data not shown), similar to our unpublished data in cell culture studies, which was attributed to the impermeability of exogenous CoQ10 across the cellular and mitochondrial membranes. Thus, we focused here on the protective effects of ALC, rather than that of CoQ10, from alcohol insult. Because the integrity of the neurofilaments was affected by alcohol ingestion, we determined the susceptibility of specific types of neurons to chronic alcohol in take. Here, we identified the loss of dopaminergic neurons by loss of fluorescence in TH protein and cholinergic neurons by the loss of fluorescence in ChAT in coronal sections of the brain. Our findings

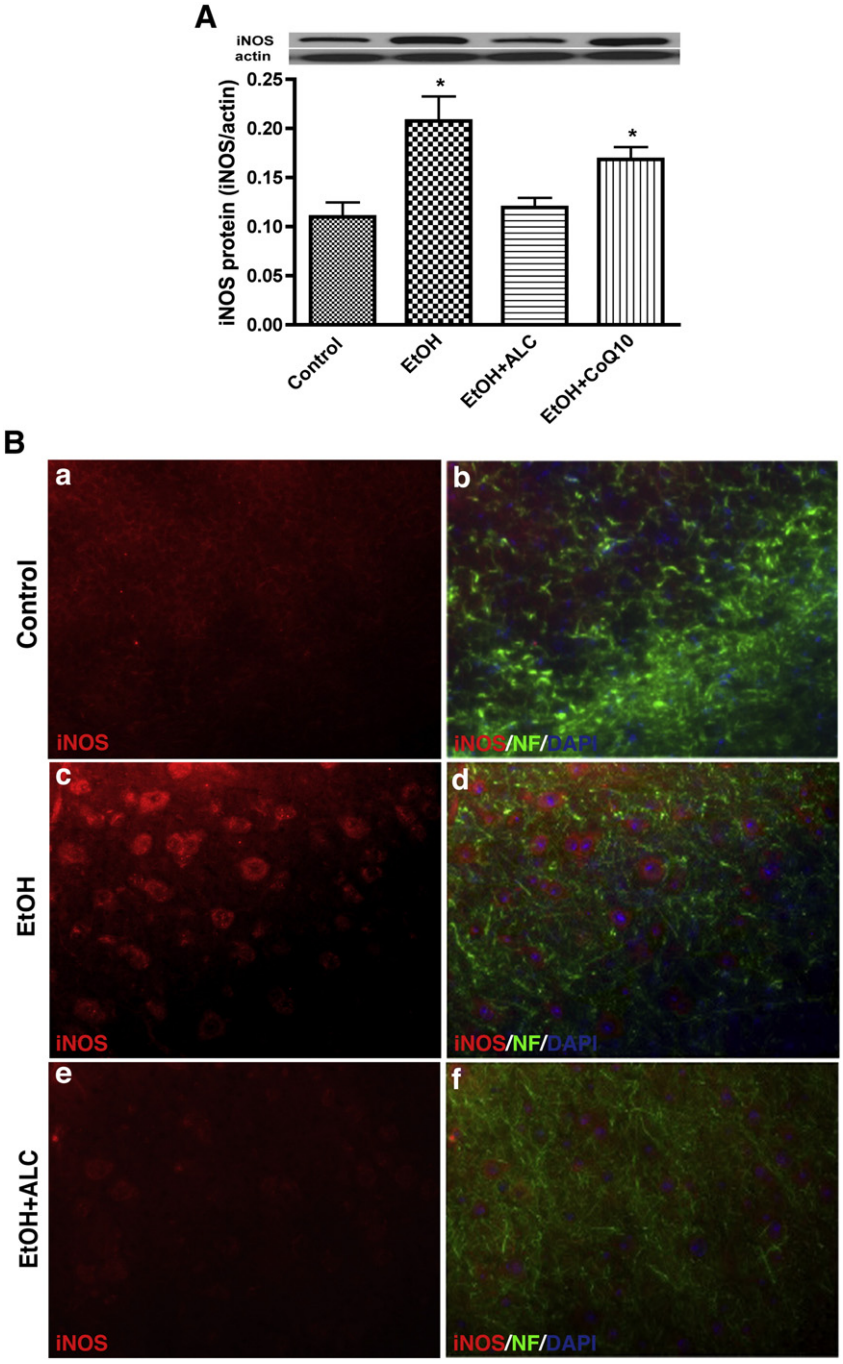

Fig. 3. Alcohol-induced iNOS protein colocalized with neurofilaments in brain frontal cortex. Protein extracts derived from the frontal cortex were analyzed for alterations in iNOS protein content, whereas coronal tissue sections were analyzed for iNOS subcellular distribution. (A) Immunoreactive bands of iNOS and actin, and quantitative iNOS protein content. Results are expressed as the ratio of iNOS to that of actin bands and presented as mean values (±SD; $n=4$). *Statistically significant ($p<0.01$) compared with controls. iNOS (rabbit IgG, 1:1000, Abcam ab3523) was used as primary antibody. (B) Double immunohistochemistry of iNOS protein and neuronal marker neurofilament (NF) in frontal cortex. iNOS (red) colocalized with NF (green) and DAPI (blue) in control (a, b), EtOH (c, d), and EtOH + ALC (e, f). iNOS (rabbit IgG, 1:50, Abcam ab3523) and NF (mouse IgG, 1:100, Abcam ab28029) were used as primary antibodies. Alexa Fluor 488 anti-mouse for neurofilaments and Alexa Fluor 594 anti-rabbit for iNOS were used as secondary antibodies. Original magnification, ×20.

revealed that dopaminergic neurons, mostly localized in the substantia nigra region, exhibited degeneration after ethanol administration (Figs. 2D–F). Similarly, cholinergic neurons detected in the outer region of the brain striatum in ethanol-fed mice were less distinct compared with control and ALC + EtOH-fed mice (Figs. 2G–I). Coadministration of ALC seemed to protect both dopaminergic and cholinergic neurons from alcohol insults in this region.

In agreement with our recent in vitro findings, we observed a twofold increase in the intensity of the 135-kDa iNOS protein in the frontal cortex after chronic alcohol ingestion compared with controls (Fig. 3A). Immunohistochemistry and confocal microscopy studies showed distinctive staining of neurofilaments around iNOS in the cytoplasm of neurons, particularly in brain tissues from alcohol ingestion (Fig. 3B). Coadministration of ALC with ethanol for 8 weeks significantly decreased alcohol-elicited iNOS protein induction in this brain region (Figs. 3A and B). Because the staining for neurofilaments and iNOS was localized differentially within the same cell body, we further confirmed the localization of iNOS in neurons by colocalizing with NeuN protein. Antibody to NeuN is specific to the nucleus and cytoplasm of neurons only, and our results clearly provide the evidence

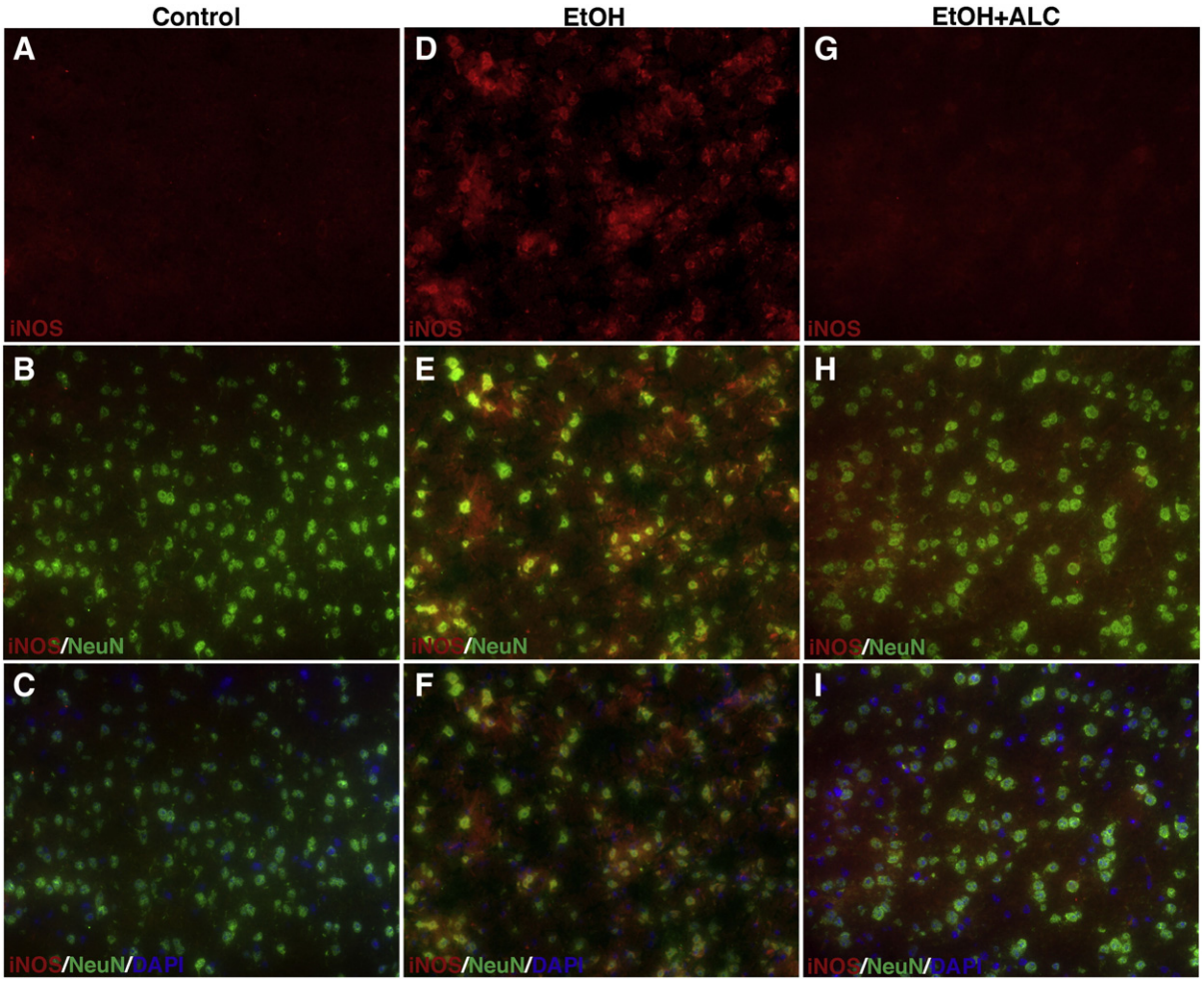

Fig. 4. Induction of iNOS in the brain perfectly colocalizes with NeuN in neuronal cell bodies. Immunofluorescence histochemical stainings of iNOS (red), NeuN (green), and DAPI nuclei (blue) in brain tissue sections. (A–C) Control brain tissue, (D–F) alcohol brain tissue, and (G–I) coadministration of alcohol and ALC in brain tissues. iNOS (rabbit IgG, 1:50, Abcam ab3523) and NeuN (mouse IgG, 1:250, Abcam ab77315) were used as primary antibodies. Alexa Fluor 488 anti-mouse for NeuN and Alexa Fluor 594 anti-rabbit for iNOS were used as secondary antibodies. Original magnification, ×20.

that iNOS was indeed perfectly colocalized with NeuN, as shown in Figs. 4A–I. Interestingly, we observed fewer neurons in brain tissues from the EtOH condition compared with the control or the ALC + EtOH condition (Figs. 4E and F).

We then examined the levels of 3-nitrotyrosine protein adducts (3-NT immunoreactivity is a signature of peroxynitrite binding to proteins). We examined their subcellular localization in frontal cortex. Antibody to 3-NT detected three immunoreactive proteins with band sizes of 25, 55, and 160 kDa. Because the immunoreactive bands for 25 and 160 kDa were very weak (bands were not accurately quantifiable after minimizing background), we present the data obtained from the 55-kDa immunoreactive protein band. We found that ethanol administration caused a 2.3-fold increase in the 3-NT protein level, which paralleled a significant induction of 3-NT protein staining that was, again, distinctly colocalized with the neuronal marker NeuN, suggesting that 3-nitrotyrosine protein adducts were formed because of iNOS induction (Figs. 5A and B). Unlike CoQ10, administration of ALC significantly blocked the ethanol-elicited up-regulation of 3-NT protein to levels that approached those of controls. These results confirm our recent findings that EtOH/Ach caused a 45% induction of iNOS protein level in primary human neurons [17]. As a positive control for 3-NT formation, brain tissue slices from control animals were incubated (1 h in CO_2 incubator) with an authentic peroxynitrite-generating compound, 3-morpholinosydnonimine hydrochloride (SIN-1; 300 μM), in the absence and presence of equimolar uric acid, a peroxynitrite scavenger. For the presence of uric acid condition, tissue slices were exposed to uric acid for 20 min in a CO_2 incubator before the addition of SIN-1 and uric acid was present at the time of SIN-1 treatment. As anticipated, the increased level of 3-NT protein expression after SIN-1 treatment was prevented by coadministration of uric acid (Fig. 5C).

Because iNOS induction and 3-NT formation led to neuroinflammation, we also studied the localization of 3-NT protein in astrocytes and microglia in brain tissue from ethanol-fed, their pair-fed controls, and alcohol + ALC-fed mice. Interestingly, 3-NT was weakly colocalized with the astrocytic marker protein GFAP (Figs. 6A–D), but was not detected in microglia (data not shown), suggesting that alcohol intake up-regulated iNOS mostly in neurons. However, numbers of distinctly stained microglia were higher in brain tissue from alcohol-fed animals (46 cells/μm^2) than in pair-fed control mice (10 cells/μm^2) in the same brain region (Figs. 6E and F), suggesting the development of an inflammatory process as a result of microgliosis in ethanol-fed mice.

Because iNOS induction did not seem to be a prominent source of oxidative stress in astrocytes and microglia, we examined the localization of NOX1 protein with the astrocyte marker protein GFAP and the microglia marker protein Iba1 in the frontal cortex. Immunohistochemical detection revealed an association between NOX1 activation and astroglial activation in alcohol-fed mice as evidenced by the colocalization of NOX1 protein with GFAP (Fig. 7) and Iba1 (Fig. 8). Again, ALC treatment partially neutralized the effects of alcohol on NOX1 protein expression in astrocytes and microglia.

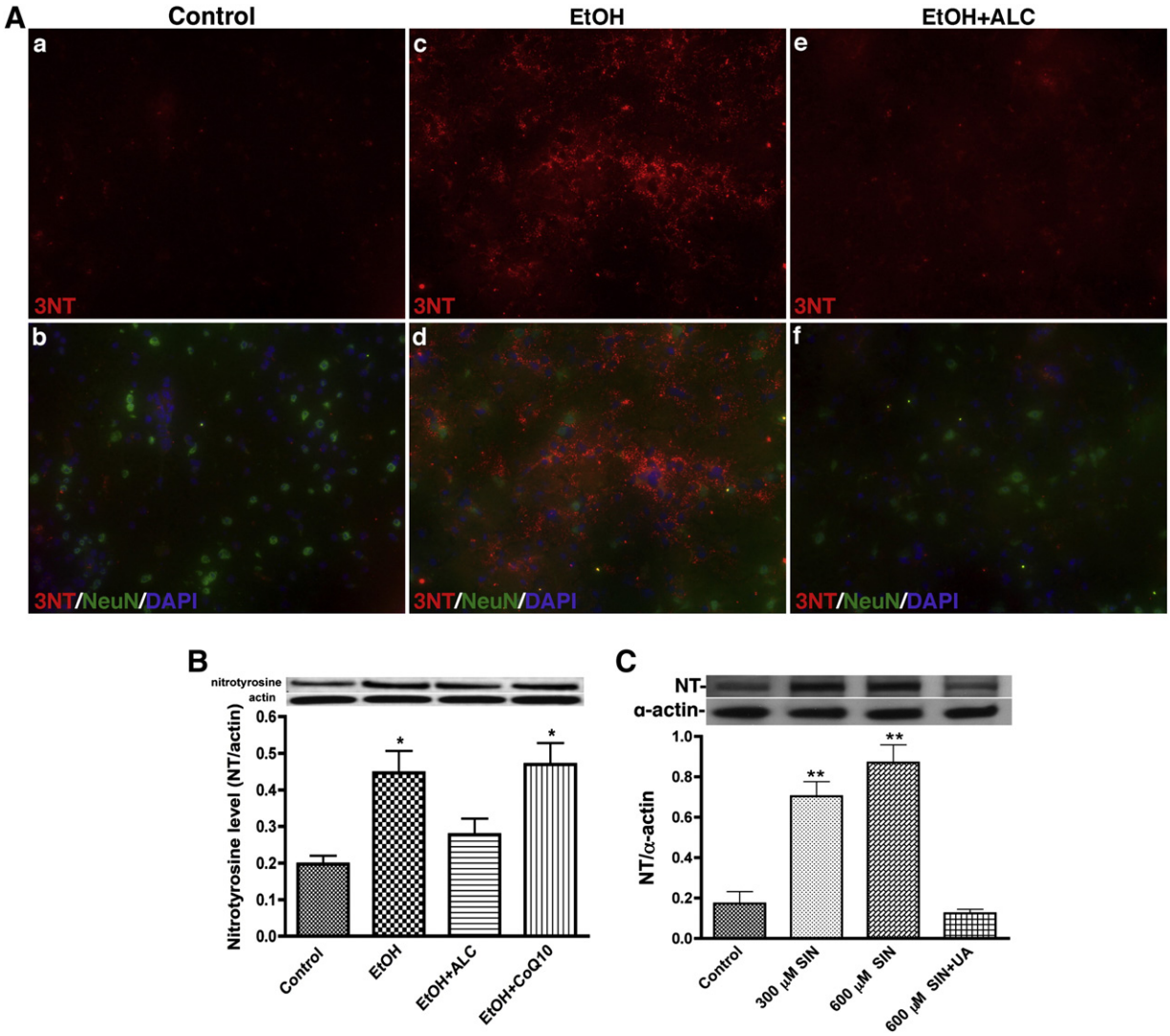

Fig. 5. Induction of iNOS correlates with increased 3-nitrotyrosine protein adduct levels in frontal cortical neurons. Protein extracts were examined for changes in 3-NT protein content, whereas tissue sections were used for 3-NT subcellular localization. (A) 3-NT protein adducts (detected by 3-nitrotyrosine antibody) colocalized with NeuN (neuronal antibody). Fluorescent stain for NeuN protein (green), 3-NT protein (red), and DAPI (blue) is shown in control (a, b), EtOH (c, d), and EtOH + ALC (e, f). 3-NT (rabbit IgG, 1:200, Abcam ab78406) and NeuN (mouse IgG, 1:250, Abcam ab77315) were used as primary antibodies. Alexa Fluor 488 anti-mouse for NeuN and Alexa Fluor 594 anti-rabbit for 3-NT were used as secondary antibodies. Original magnification, ×20. (B) Immunoreactive bands of 3-NT and actin, and quantitative 3-NT protein content. Results are expressed as the ratio of 3-NT protein adduct to actin bands and presented as mean values (±SD; $n=4$). *Statistically significant ($p<0.01$) compared with control. (C) Immunoreactive bands of 3-NT-protein adduct and actin in SIN-1-treated brain tissue samples and quantitative 3-NT protein content. Results are expressed as the ratio of 3-NT to actin bands and presented as mean values (±SD; $n=3$). 3-NT (mouse IgG, 1:1000, Abcam ab52309) was used as primary antibody. **Statistically significant ($p<0.01$) compared with control.

To assess the association between NOX1 activation and oxidative damage in the brain, we then evaluated the changes in NOX1 protein level and formation of the ROS-mediated lipid peroxidation product 4-HNE. Antibody to NOX1 detected multiple immunoreactive bands with a prominent band size of approximately 65 kDa, which was the expected molecular weight of NOX1 protein. Ethanol administration caused a 2.5-fold increase in the intensity of the 65-kDa NOX1-immunoreactive band in brain tissues compared with brains from pair-fed controls (Fig. 9A). Elevation in NOX1 protein level was accompanied by a 2.8-fold increase in 4-HNE protein adduct content in alcohol-fed mice compared with controls (Fig. 9B). Coadministration of ALC (but not malonyl coenzyme A or CoQ10) almost completely abrogated the up-regulation by alcohol of NOX1 and 4-HNE protein in the brain. To verify the formation of 4-HNE (a signature of ROS oxidatively damaged proteins), we measured ROS production by a direct electron paramagnetic resonance method in this brain region. These analyses confirmed our findings with 4-HNE that chronic alcohol ingestion significantly enhanced the production of ROS, and, interestingly, ALC diminished ROS generation (Fig. 9C). Thus, our findings indicate that ALC neutralizes oxidative damage in the brain caused by chronic ethanol administration.

Discussion

In previous studies, we found that the mortality of mice (C57BL/6J) increased at week 4 or 5 when the ethanol concentration in the liquid diet was higher than 4% (vol/vol). Thus, in this study, we avoided such mortality by feeding mice ethanol as 28% of total calories (4% wt/vol) in the liquid diet for 8 weeks. This concentration is considered a high ethanol dose in mice. Blood alcohol levels were 10.6–17.6 mM (0.05–0.1%). Although brain alcohol level was not determined in this study, we surmise a range similar to that of the blood level because ethanol easily crosses the blood–brain barrier. This was demonstrated by the report of Griffin et al. [25] in which a blood alcohol level of 27.7–36.4 mM was similar to the brain alcohol level of 28.4–35.4 mM in mice after either voluntary drinking or exposure to ethanol vapor. Despite the modest body weight gain, the loss of brain tissue weight in the alcohol groups was attributed to

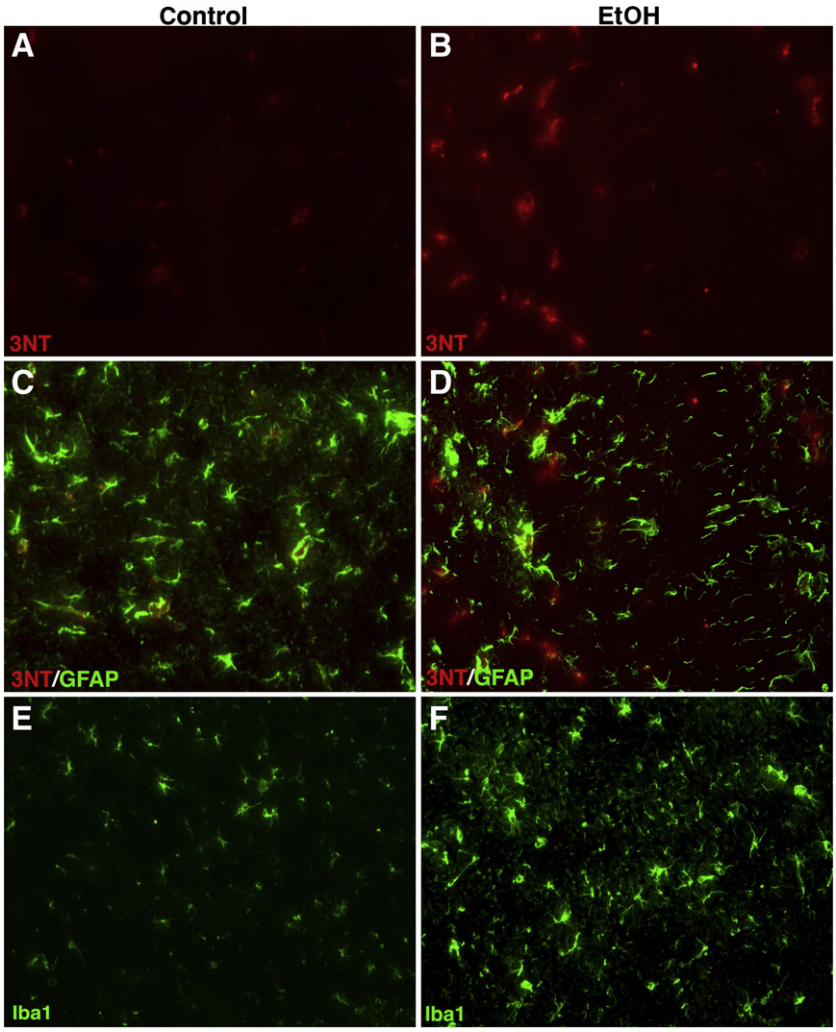

Fig. 6. Detection of nitrotyrosine immunoreactivity in frontal cortical astrocytes. (A–D) Brain frontal tissue sections were stained for 3-NT protein adducts (red) and merged with the astrocyte-specific protein marker GFAP (green). (A) 3-NT in control tissue, (B) 3-NT in alcoholic tissue, (C) colocalization of 3-NT and GFAP proteins in control, (D) colocalization of 3-NT and GFAP proteins in brains of alcohol-fed mice. 3-NT (mouse IgG, 1:200, Abcam ab61392) and GFAP (rabbit IgG, 1:250, Abcam ab7260) were used as primary antibodies. Alexa Fluor 488 anti-rabbit for GFAP and Alexa Fluor 594 anti-mouse for 3-NT were used as secondary antibodies. (E, F) The brain frontal tissue sections from control and alcohol -fed mice were stained for the microglia marker Iba1 (green). (E) Iba1 in control tissue, (F) Iba1 in alcoholic tissue. Goat IgG Iba1 (1:100, Abcam ab5076) was used as primary antibody. Alexa Fluor 488 anti-goat was used for Iba1 as secondary antibody. Original magnification, ×20.

brain shrinkage due to loss of white and gray matter, which has been documented in chronic alcohol abusers [26,27].

The significance of the present findings is that chronic alcohol feeding activated ROS- and RNS-generating pathways in specific brain cell types. The induction of oxidative damage and activation of inflammatory response in these different cell types abrogated the loss of neurons and long-term potentiation of synaptic neurotransmission in the frontal cortex. We noted that timely administration of ALC significantly stabilized the long-term synaptic neurotransmission of dopaminergic and cholinergic neurons by preventing the activation of iNOS, NOX, and glial cells.

It was anticipated that an increase in iNOS protein would correlate with an up-regulation of 3-nitrotyrosine protein levels in the frontal cortex of ethanol-fed mice. Colocalization of neurofilaments and iNOS protein confirmed that iNOS was mostly expressed in neurons around a single or a couple of nuclear membranes. Detection of iNOS (NOS2) protein in the pair-fed controls may be due to cross-reaction of iNOS antibody with the constitutive nNOS (NOS1) protein, which was apparent by the similar nuclear membrane staining pattern of nNOS in brain tissue sections (data not shown). Remarkably, neither astrocytes nor microglia exhibited colocalization of iNOS/3-NT in this brain region, further confirming not only that iNOS induction is a major source of peroxynitrite, but also that the enzyme is not responsive in astrocytes and microglia. These findings indicate that chronic alcohol ingestion preferentially modulates iNOS protein level in neurons but not in astrocytes or microglia, validating our recent findings that EtOH/Ach exposure increased the level of iNOS protein in cultured primary human neurons [17]. Apart from these findings, Konovko et al. [28] reported an induction of iNOS in cerebellar cortical neurons; however, induction of iNOS in cerebral neurons by chronic alcohol consumption had been only rarely documented in the literature. We conclude that iNOS induction led to accumulation of NO and peroxynitrite formation thereby promoting the transduction of oxidative stress and neuronal degeneration during chronic ethanol consumption.

Although we observed that ethanol-elicited iNOS induction was specific to neurons, the increase in NOX level, which produces ROS, and 4-HNE formation correlated with a colocalization of NOX protein, which was specific to astrocytes and microglia. Nitric oxide freely diffuses across biological membranes, whereas endogenously formed ROS (superoxide and hydroxyl radicals) do not cross the cell membrane. This implies that NO generated by neurons diffuses into

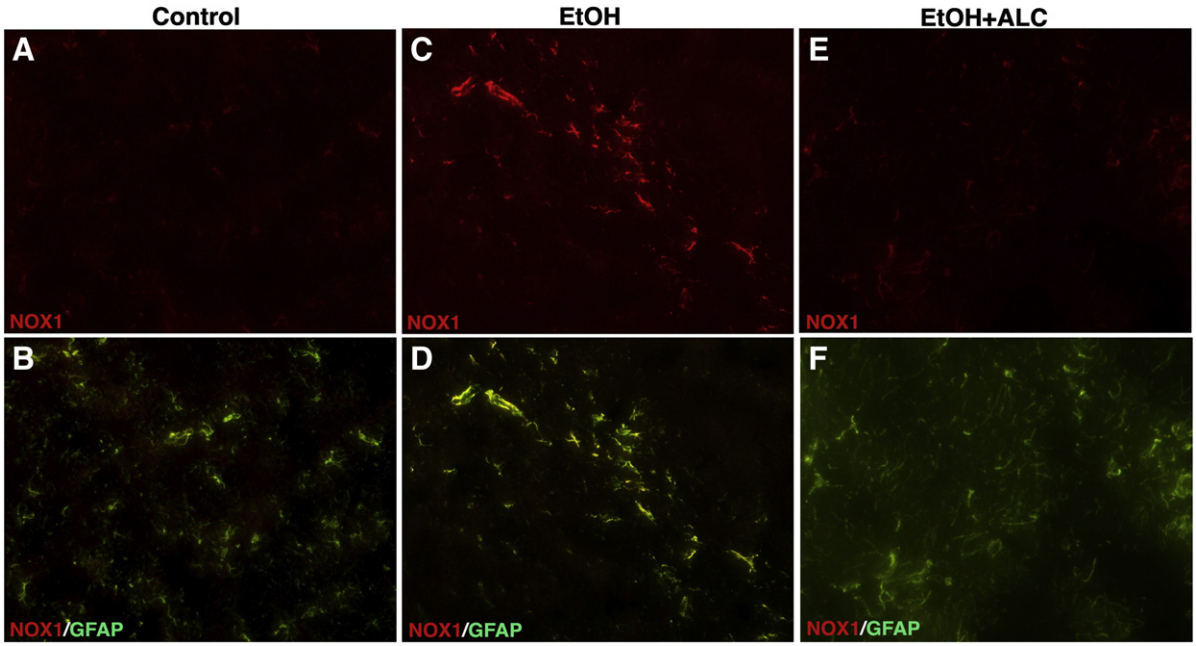

Fig. 7. NOX1 protein colocalized with astrocytes (GFAP) in the frontal cortex. Double immunohistochemistry of GFAP (green) with NOX1 (red) protein (A, B) in control brain tissue, (C, D) in alcohol brain tissue, and (E, F) in coadministration of alcohol and ALC brain tissues. NOX1 (rabbit IgG, 1:150, Abcam ab55831) and GFAP (mouse IgG, 1:250, Abcam ab10062) were used as primary antibodies. Alexa Fluor 488 anti-mouse for GFAP and Alexa Fluor 594 anti-rabbit for NOX1 were used as secondary antibodies. Original magnification, ×20.

glial cells and reacts with superoxide to form highly reactive peroxynitrite. This would cause oxidative stress and an inflammatory response in glial cells as indicated by gliosis after alcohol abuse. In neuronal cells, excess production of NO is expected to shift the chemistry into pronitrosative conditions. However, leakage of ROS from neuronal mitochondria may favor the formation of peroxynitrite within neurons. Formation of peroxynitrite either in glial cells or in neurons can then exacerbate physiological damage as observed in alcohol-exposed brain endothelial cells [17,29] or in livers of ethanol-fed rodents [30]. Most importantly, ALC significantly minimized the level of alcohol-induced iNOS/nitrotyrosine adduct formation in neurons and further prevented NOX protein induction in astrocytes and microglia, thereby preventing gliosis in the frontal cortex. These findings indicated that ALC, by providing carnitine and acetyl groups,

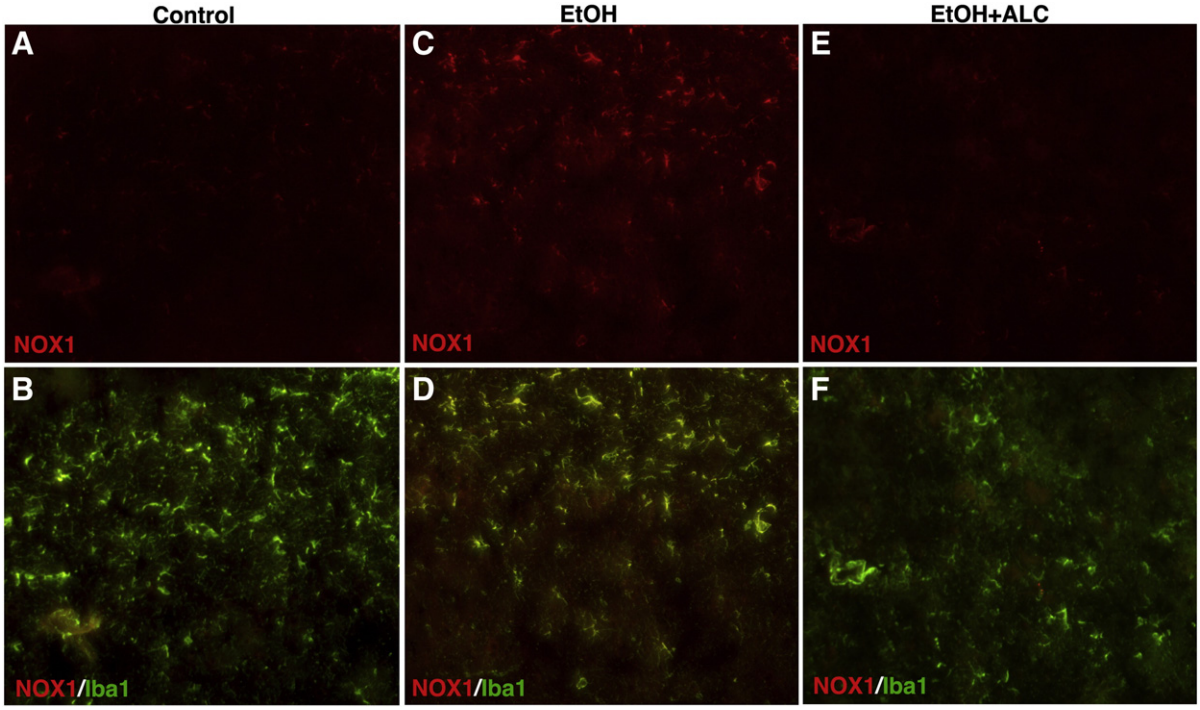

Fig. 8. Brain frontal cortex tissue sections from chronic studies were stained for colocalization of NOX1 (red) protein with microglia (Iba1; green). (A) Control, (C) EtOH, and (E) EtOH + ALC; NOX1 alone. (B) Control, (D) EtOH, and (F) EtOH + ALC, colocalization of NOX1 with microglia. Microglia were immunolabeled with antibody to Iba1 (goat IgG, 1:100) or NOX1 (rabbit IgG, 1:200) for 1 h at 24 °C. NOX1 (rabbit IgG, 1:150, Abcam ab55831) and Iba1 (goat IgG, 1:100, Abcam ab5076) were used as primary antibodies. Alexa Fluor 488 anti-goat for Iba1 and Alexa Fluor 594 anti-rabbit for NOX1 were used as secondary antibodies. Original magnification, ×20.

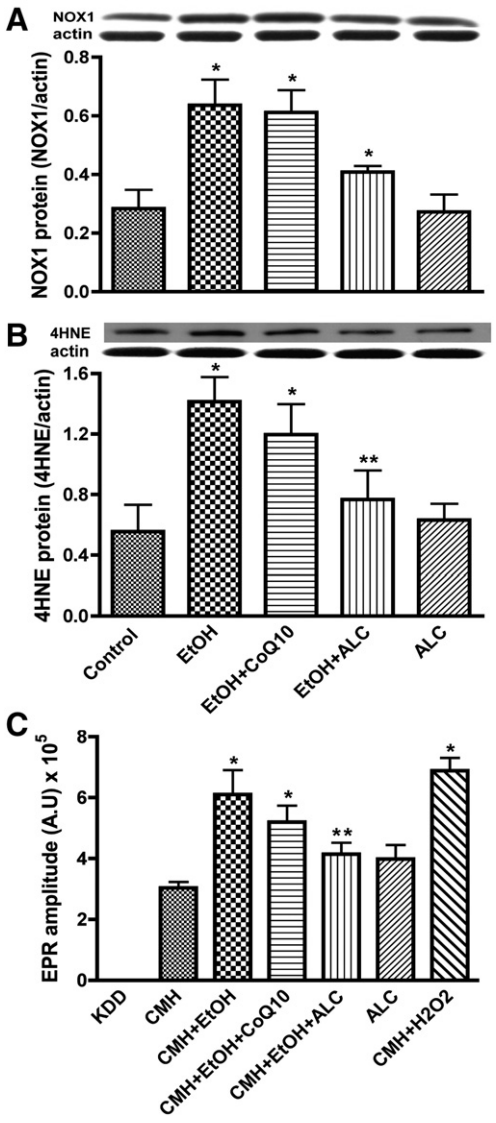

Fig. 9. Detection of NOX1, 4-HNE, and ROS in brain tissue samples. Brain homogenate protein extracts from chronic ethanol liquid diet-fed or pair-fed control mice were analyzed for changes in NOX1 protein and 4-HNE protein. (A) Immunoreactive bands of NOX1 (65 kDa) and actin and NOX1 protein content. NOX1 (rabbit IgG, 1:200, Abcam ab55831) was used as primary antibody. (B) Immunoreactive bands of 4-HNE and actin and 4-HNE protein level. Results are expressed as the ratio of NOX1 or 4-HNE to actin bands and presented as mean values (±SD; $n=4$). 4-HNE (rabbit IgG, 1:1000, Alpha Diagnostic HNE11-S) was used as primary antibody. (C) ROS generation was detected by electron paramagnetic resonance (EPR) in brain tissue slices from chronic ethanol-fed or pair-fed control mice. H_2O_2 (50 μM) was used as a positive control that was added to control brain tissue slices 30 min before EPR detection. Results are expressed in EPR amplitude arbitrary units and presented as mean values (±SD; $n=4$). *Statistically significant ($p<0.01$) compared with controls. **Statistically significant ($p<0.01$) compared with alcohol condition.

has therapeutic value as an antioxidant and anti-inflammatory agent. However, ALC is not a direct scavenger of free radicals (ROS or RNS). Thus, we postulate that ALC exerts its antioxidant property by indirect mechanisms such as its ability to maintain mitochondrial membrane potential transition. One possible mechanism by which ALC could act is by suppressing the activation of free radical-generating pathways such as iNOS and NOX as indicated by the present findings. The molecular mechanism of suppressing iNOS and NOX activation by ALC in the CNS warrants further investigation. Another plausible mechanism for ALC to circumvent the excessive level of oxidative stress is to stabilize the naturally occurring biological antioxidant enzymes and antioxidants such as SOD, catalase, or the intracellular levels of glutathione. In fact, Mansour [31] reported that a high dose (250 mg/kg body wt) of ALC significantly increase glutathione peroxidase and SOD activities in the lungs and livers of rodents, and Calabrese et al. [32] demonstrated the induction of heme oxygenase-1, Hsp70, and SOD-2 by ALC, suggesting that ALC can act as an antioxidant by inducing these antioxidant enzymes. It is now widely accepted that oxidative damage and inflammation contribute to white and gray matter injury in the brain [33]. Thus, minimizing oxidative damage could alleviate the inflammatory response because oxidative stress has been linked to initiation of neuroinflammation [10]. Such was the case in this study, that the numbers of microglia in alcoholic brain were higher than those in mice given ALC plus alcohol or in the pair-fed controls. Whether ALC prevented the infiltration of leukocytes into the brain or maturation and homing of microglia in the CNS remains to be investigated. These studies established the link between oxidative stress and inflammatory response in specific cell types in the brain during chronic alcohol ingestion, validating our recent findings that ethanol metabolism causes a significant induction of iNOS protein level in primary human neurons [17].

An equally important finding was the stabilization of the LFS and LTP synaptic transmission by ALC in the frontal cortex after chronic alcohol ingestion. It must be noted here that these data demonstrated the actual physiological decaying pattern of neuronal transmission in chronic alcohol consumption without any *stimulating* or *antagonizing* agent at the time of electrophysiological recording. Under this ex vivo condition without agonist or antagonist, the LTP transmission of all experimental conditions was expected to overlap with time to the basal level because of a decrease in neuronal viability. Although the neurotransmission of ALC + EtOH decayed faster than that of the pair-fed control, the protective effect of ALC from chronic alcohol abuse was visible and statistically significant for the first 30-min time point. This finding suggested that, although ALC provided neuroprotection, it was unable to inhibit the sensitivity to chronic alcohol insult completely.

Because synaptic transmission is a highly energy-dependent process, stabilization of neurotransmission by ALC after long-term alcohol consumption may be associated with protection of neuronal mitochondrial function. In particular, the ability of ALC to prevent alcohol-induced mitochondrial damage, energy depletion due to defective respiratory chain complexes, oxidative-mediated neuroinflammation, and neuronal degeneration will be of significant importance in further investigations. Indeed, during chronic alcohol consumption, ALC sustained the neuronal LFS and LTP synaptic transmission by preserving the integrity of neurofilaments and by maintaining dopaminergic and cholinergic neurons. These findings lead us to suggest that ALC regulates the activation of the acetylcholine receptor, as the acetyl group is an essential precursor for the neurotransmitter acetylcholine. Because alcohol is a legalized substance of abuse and there are few pharmacological treatments for alcohol-induced brain injury, we propose that daily use of dietary ALC (1–2 mg/kg body wt) by alcohol abusers could provide a potential health benefit. The significance of this proposal originated from the fact that ALC is already in clinical use as a therapeutic agent for treatment of neurological diseases.

Acknowledgment

This work was supported in part by NIH/NIAAA Grant AA016403-01A2 (to J.H.) and by the UNMC Faculty Retention Fund.

References

[1] Parsons, O. A. Neurocognitive deficits in alcoholics and social drinkers: a continuum? *Alcohol. Clin. Exp. Res.* **22:**954–961; 1998.
[2] Zeigler, D. W.; Wang, C. C.; Yoast, R. A.; Dickinson, B. D.; McCaffree, M. A.; Robinowitz, C. B.; Sterling, M. L. The neurocognitive effects of alcohol on adolescents and college students. *Prev. Med.* **40:**23–32; 2005.

[3] Harper, C. The neuropathology of alcohol-specific brain damage, or does alcohol damage the brain? *J. Neuropathol. Exp. Neurol.* **57:**101–110; 1998.
[4] Lin, M. T.; Beal, M. F. Mitochondrial dysfunction and oxidative stress in neurodegenerative diseases. *Nature* **443:**787–795; 2006.
[5] Maracchioni, A.; Totaro, A.; Angelini, D. F.; Di Penta, A.; Bernardi, G.; Carri, M. T.; Achsel, T. Mitochondrial damage modulates alternative splicing in neuronal cells: implications for neurodegeneration. *J. Neurochem.* **100:**142–153; 2007.
[6] Crews, F. T.; Collins, M. A.; Dlugos, C.; Littleton, J.; Wilkins, L.; Neafsey, E. J.; Pentney, R.; Snell, L. D.; Tabakoff, B.; Zou, J.; Noronha, A. Alcohol-induced neurodegeneration: when, where and why? *Alcohol. Clin. Exp. Res.* **28:**350–364; 2004.
[7] Baydas, G.; Tuzcu, M. Protective effects of melatonin against ethanol-induced reactive gliosis in hippocampus and cortex of young and aged rats. *Exp. Neurol.* **194:**175–181; 2005.
[8] Pierce, D. R.; Cook, C. C.; Hinson, J. A.; Light, K. E. Are oxidative mechanisms primary in ethanol induced Purkinje neuron death of the neonatal rat? *Neurosci. Lett.* **400:**130–134; 2006.
[9] Riikonen, J.; Jaatinen, P.; Rintala, J.; Porsti, I.; Karjala, K.; Hervonen, A. Intermittent ethanol exposure increases the number of cerebellar microglia. *Alcohol Alcohol.* **37:**421–426; 2002.
[10] Potula, R.; Haorah, J.; Knipe, B.; Leibhart, J.; Chrastil, J.; Heilman, D.; Dou, H.; Reddy, R.; Ghorpade, A.; Persidsky, Y. Alcohol abuse enhances neuroinflammation and impairs immune responses in an animal model of human immunodeficiency virus-1 encephalitis. *Am. J. Pathol.* **168:**1335–1344; 2006.
[11] He, J.; Crews, F. T. Increased MCP-1 and microglia in various regions of the human alcoholic brain. *Exp. Neurol.* **210:**349–358; 2008.
[12] Blanco, A. M.; Guerri, C. Ethanol intake enhances inflammatory mediators in brain: role of glial cells and TLR4/IL-1RI receptors. *Front. Biosci.* **12:**2616–2630; 2007.
[13] Crews, F. T.; Nixon, K. Mechanisms of neurodegeneration and regeneration in alcoholism. *Alcohol Alcohol.* **44:**115–127; 2009.
[14] Sullivan, E. V.; Zahr, N. M. Neuroinflammation as a neurotoxic mechanism in alcoholism: commentary on "Increased MCP-1 and microglia in various regions of human alcoholic brain.". *Exp. Neurol.* **213:**10–17; 2008.
[15] Haorah, J.; Heilman, D.; Knipe, B.; Chrastil, J.; Leibhart, J.; Ghorpade, A.; Miller, D. W.; Persidsky, Y. Ethanol-induced activation of myosin light chain kinase leads to dysfunction of tight junctions and blood–brain barrier compromise. *Alcohol. Clin. Exp. Res.* **29:**999–1009; 2005.
[16] Haorah, J.; K.B.; Gorantla, S.; Zheng, J.; Persidsky, Y. Alcohol-induced blood–brain barrier dysfunction is mediated via inositol 1,4,5-triphosphate receptor IP3R-gated intracellular calcium release. *J. Neurochem.* **100:**324–336; 2007.
[17] Haorah, J.; R.S.; Floreani, N.; Gorantla, S.; Morsey, B.; Persidsky, Y. Mechanism of alcohol-induced oxidative stress and neuronal injury. *Free Radic. Biol. Med.* **45:** 1542–1550; 2008.
[18] Montoliu, C.; Sancho-Tello, M.; Azorin, I.; Burgal, M.; Valles, S.; Renau-Piqueras, J.; Guerri, C. Ethanol increases cytochrome P4502E1 and induces oxidative stress in astrocytes. *J. Neurochem.* **65:**2561–2570; 1995.
[19] Colton, C. A.; Snell-Callanan, J.; Chernyshev, O. N. Ethanol induced changes in superoxide anion and nitric oxide in cultured microglia. *Alcohol. Clin. Exp. Res.* **22:** 710–716; 1998.
[20] Lolic, M. M.; Fiskum, G.; Rosenthal, R. E. Neuroprotective effects of acetyl-L-carnitine after stroke in rats. *Ann. Emerg. Med.* **29:**758–765; 1997.
[21] Pettegrew, J. W.; Klunk, W. E.; Panchalingam, K.; Kanfer, J. N.; McClure, R. J. Clinical and neurochemical effects of acetyl-L-carnitine in Alzheimer's disease. *Neurobiol. Aging* **16:**1–4; 1995.
[22] Hagen, T. M.; Ingersoll, R. T.; Wehr, C. M.; Lykkesfeldt, J.; Vinarsky, V.; Bartholomew, J. C.; Song, M. H.; Ames, B. N. Acetyl-L-carnitine fed to old rats partially restores mitochondrial function and ambulatory activity. *Proc. Natl. Acad. Sci. U. S. A.* **95:**9562–9566; 1998.
[23] Piovesan, P.; Quatrini, G.; Pacifici, L.; Taglialatela, G.; Angelucci, L. Acetyl-L-carnitine restores choline acetyltransferase activity in the hippocampus of rats with partial unilateral fimbria–fornix transection. *Int. J. Dev. Neurosci.* **13:**13–19; 1995.
[24] Xiong, H.; Baskys, A.; Wojtowicz, J. M. Brain-derived peptides inhibit synaptic transmission via presynaptic GABAB receptors in CA1 area of rat hippocampal slices. *Brain Res.* **737:**188–194; 1996.
[25] Griffin III, W. C.; Lopez, M. F.; Yanke, A. B.; Middaugh, L. D.; Becker, H. C. Repeated cycles of chronic intermittent ethanol exposure in mice increases voluntary ethanol drinking and ethanol concentrations in the nucleus accumbens. *Psychopharmacology (Berlin)* **201:**569–580; 2009.
[26] Harper, C.; Dixon, G.; Sheedy, D.; Garrick, T. Neuropathological alterations in alcoholic brains: studies arising from the New South Wales Tissue Resource Centre. *Prog. Neuropsychopharmacol. Biol. Psychiatry* **27:**951–961; 2003.
[27] Harper, C.; Kril, J. If you drink your brain will shrink: neuropathological considerations. *Alcohol Alcohol. Suppl.* **1:**375–380; 1991.
[28] Konovko, O.; Yu, E.; Morozov, Y. E.; Kalinichenko, G.; Dyuzen, V.; Motavkin, P. A. Induction of NO-synthase and acetaldehyde dehydrogenase in neurons of human cerebellar cortex during chronic alcohol intoxication. *J. Bull. Exp. Biol. Med.* **137:** 211–214; 2004.
[29] Haorah, J.; Knipe, B.; Leibhart, J.; Ghorpade, A.; Persidsky, Y. Alcohol-induced oxidative stress in brain endothelial cells causes blood–brain barrier dysfunction. *J. Leukocyte Biol.* **78:**1223–1232; 2005.
[30] Osna, N. A.; Haorah, J.; Krutik, V. M.; Donohue Jr., T. M. Peroxynitrite alters the catalytic activity of rodent liver proteasome in vitro and in vivo. *Hepatology* **40:** 574–582; 2004.
[31] Mansour, H. H. Protective role of carnitine ester against radiation-induced oxidative stress in rats. *Pharmacol. Res.* **54:**165–171; 2006.
[32] Calabrese, V.; Colombrita, C.; Sultana, R.; Scapagnini, G.; Calvani, M.; Butterfield, D. A.; Stella, A. M. Redox modulation of heat shock protein expression by acetylcarnitine in aging brain: relationship to antioxidant status and mitochondrial function. *Antioxid. Redox Signaling* **8:**404–416; 2006.
[33] Kaindl, A. M.; Favrais, G.; Gressens, P. Molecular mechanisms involved in injury to the preterm brain. *J. Child Neurol.* **24:**1112–1118; 2009.